

Communication

In-Situ TEM Study of a Nanoporous Ni–Co Catalyst Used for the Dry Reforming of Methane

Takeshi Fujita ^{1,*} , Kimitaka Higuchi ², Yuta Yamamoto ², Tomoharu Tokunaga ², Shigeo Arai ² and Hideki Abe ³

¹ Advanced Institute for Materials Research, Tohoku University, Sendai 980-8577, Japan

² Institute of Materials and Systems for Sustainability, Nagoya University, Nagoya 464-8603, Japan; k.higuchi@imass.nagoya-u.ac.jp (K.H.); y.yamamoto@imass.nagoya-u.ac.jp (Y.Y.); tokunaga.tomoharu@material.nagoya-u.ac.jp (T.T.); arai@imass.nagoya-u.ac.jp (S.A.)

³ National Institute for Materials Science, Ibaraki 305-0044, Japan; ABE.Hideki@nims.go.jp

* Correspondence: tfujita@wpi-aimr.tohoku.ac.jp; Tel.: +81-22-217-5990

Received: 24 August 2017; Accepted: 28 September 2017; Published: 1 October 2017

Abstract: We performed in-situ transmission electron microscopy (TEM) on a dealloyed nanoporous NiCo catalyst used for the dry reforming of methane (DRM) to investigate the origin of the catalytic activity and structural durability. The in-situ observations and local chemical analysis indicated that the DRM induced chemical demixing of Ni and Co accompanied by grain refinement, implying possible “synergic effects” in a general bimetallic NiCo catalyst when used for the DRM.

Keywords: nanoporous metal; methane dry reforming; in-situ TEM observation

1. Introduction

Efficient utilization of the greenhouse gases carbon dioxide (CO_2) and methane, the major components of natural gas (shale gas), is the topic of key research due to global warming. The conversion of methane and CO_2 into “syngas” ($\text{H}_2 + \text{CO}$) via dry reforming of methane (DRM), which can be represented by the equation $\text{CH}_4 + \text{CO}_2 \rightarrow 2\text{H}_2 + 2\text{CO}$, could be one technological solution to the problem of high methane and CO_2 levels [1–3]. The dry reforming reaction is typically accompanied by the simultaneous occurrence of the reverse water–gas shift reaction, $\text{CO}_2 + \text{H}_2 \rightarrow \text{CO} + 2\text{H}_2\text{O}$. A variety of catalysts have been evaluated for DRM; however, the reaction typically requires a high temperature (550–1000 °C), causing significant catalyst degradation due to sintering of materials and coke deposition. Although many (typically Ni-based) heterogeneous catalysts have had their stabilities and performances evaluated, there have been few far-reaching advances in the understanding of the reactions and the enhancement of catalyst stability due to the lack of structural evaluation being used.

Recently, the development of nanoporous metals by dealloying has established an intriguing functional-material platform, with applications now expanding into multi-discipline fields related to batteries, catalysis, sensing, and biotechnology applications [4–8]. As a gas-conversion catalyst, nanoporous gold has been studied as a single-component benchmark material and systematically investigated for CO oxidation [9], but the thermal degradation of pores and ligament coarsening due to surface diffusion/migration results in significant losses of catalytic activity [10]. In order to improve thermal stability, a thermal-resistant nanoporous composite was proposed: nanoporous CuNiMnO has been fabricated by leaching Mn from a CuNiMn alloy precursor [11]. The resulting material was durable and catalytically active toward both NO reduction and CO oxidation at 400 °C for 10 days, as the thermal-resistant nanostructure was activated by the reactions due to the tangled active metal and thermally stable oxide network. However, DRM requires a higher reaction temperature than CO oxidation and NO reduction, and therefore demands more thermal stability, but the potential use of nanoporous metal-based catalysts for this reaction is totally unknown.

In this study, we evaluated the DRM performance of nanoporous metals (NP-Ni, NP-NiCo, and NP-Co) by dealloying NiMn, NiCoMn, and CoMn precursor alloys, and found that the addition of Co enhanced the thermal stability with moderate activity. We then employed in-situ transmission electron microscopy (TEM) of a nanoporous NiCo during DRM to investigate the reason for the increased thermal stability.

2. Materials and Methods

$\text{Ni}_{15}\text{Co}_{15}\text{Mn}_{70}$, $\text{Ni}_{30}\text{Mn}_{70}$, and $\text{Co}_{30}\text{Mn}_{70}$ (at %) ingots were prepared by melting pure Ni, Co, and Mn (purity >99.9 at %) using an Ar-protected arc melting furnace. We had already fabricated NP-Ni in sheet form in a previous study [12]. Briefly, after annealing $\text{Ni}_{30}\text{Mn}_{70}$ at 900 °C under Ar to provide microstructure and composition homogenization, the ingots were cold-rolled into ~50-μm-thick sheets at room temperature. For NP-NiCo and NP-Co, alloy ribbons of $\text{Ni}_{15}\text{Co}_{15}\text{Mn}_{70}$ and $\text{Co}_{30}\text{Mn}_{70}$ with thicknesses of ~25–30 μm were prepared using an induction melt spinning method. These alloy sheets/ribbons were dealloyed in a 1 M $(\text{NH}_4)_2\text{SO}_4$ solution at 50 °C for 5 h. After dealloying, the samples were rinsed thoroughly with water and ethanol and dried under vacuum.

The as-made nanoporous samples were mechanically brittle, and the samples were gently crushed into a powder with particle diameters of 100–200 μm. The crushed samples (100 mg) were loaded into a 4-mm quartz tube and tested in a continuous-flow fixed-bed microreactor in a catalysis system (BELCAT, MicrotracBEL, Osaka, Japan) at atmospheric pressure. The amounts of H_2 , CH_4 , CO, and CO_2 were monitored and evaluated with an on-line gas analyzer (BELMass, MicrotracBEL, Osaka, Japan), with a reactant gas containing 0.8% CH_4 , 0.8% CO_2 , and He for balance being introduced into the reactor at a flow rate of $10 \text{ cm}^3 \cdot \text{min}^{-1}$. The samples were ramped up to 650 °C at a rate of $2 \text{ }^\circ\text{C} \cdot \text{min}^{-1}$.

The microstructures were characterized using a scanning electron microscope (SEM, JSM-6700, JEOL, Tokyo, Japan) and transmission electron microscope (JEM-2100F, JEOL, Tokyo, Japan) equipped with aberration correctors (CEOS GmbH, Heidelberg, Germany) for the image- and probe-forming lens systems, as well as an energy dispersive X-ray spectrometry (EDS) system (JED-2300T, JEOL, Tokyo, Japan) for chemical composition analysis. A probe convergence angle of 29 mrad and a high-angle annular dark-field (HAADF) detector with an inner angle of greater than 100 mrad were used for HAADF-scanning TEM (STEM). The samples were transferred onto a holey carbon grid on Cu mesh without a uniform carbon support film (JEOL catalog no. 7801 11613, Tokyo, Japan). SEM analysis was conducted at an accelerating voltage of 15.0 kV.

For in-situ TEM, we used a dedicated 1000 kV JEM-1000K RS TEM (JEOL, Tokyo, Japan) equipped with an environmental cell specially designed at Nagoya University, Japan [13]. The samples were heated up to 600 °C under vacuum and observed in the presence of a $\text{CH}_4 + \text{CO}_2$ gas mixture (1 vol % CH_4 , 1 vol % CO_2 , and 98 vol % Ar) at 600 °C over a wide range of total pressures (1–30 Pa). A furnace-type heating holder (JEOL, EM-Z083171STHH, Tokyo, Japan) was used. It would be relevant to mention that due to the pressure dependence of DRM, using lower pressures results in higher conversion of CH_4 and CO_2 [14]. The electron beam current flux was $0.23 \text{ A} \cdot \text{cm}^{-2}$, as measured with a Faraday gauge. The nanostructure was very stable under electron beam irradiation both under vacuum and in a pure Ar atmosphere. Detectable changes in the structure were vividly observed from the start of catalysis when the reaction gases were delivered into the environmental cell. In addition, DRM is an endothermic reaction. Therefore, when the sample stage in the TEM is heated up, the sample temperature tended to decrease if we did not increase the output of the heating stage. These factors demonstrate that the self-transformation of the nanostructure was mainly driven by the catalytic reaction.

3. Results and Discussion

The evolution of H_2 by the three samples (NP-Ni, NP-NiCo, and NP-Co) and the change in temperature over time are shown in Figure 1. NP-Ni showed a rapid generation of H_2 at ~500 °C, but

this began to drop rapidly at 550 °C, indicating poor thermal stability. Unexpectedly, NP-Co showed inert activity, suggesting a possible oxidation of the metal [15] and reduced activity of Co compared to Ni [16]. Interestingly, NP-NiCo showed moderate thermal stability and maintained activity up to 650 °C, whereas NP-Ni was unstable.

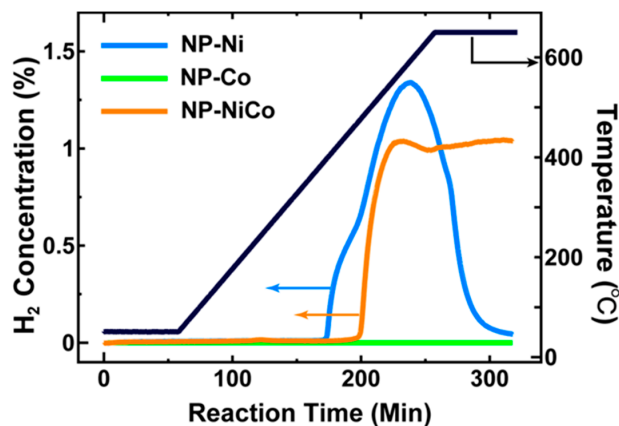


Figure 1. Concentrations of H₂ in outlet gases for NP-Ni, NP-Co, and NP-NiCo samples, as well as the change in temperature over time.

The microstructures of the three samples before and after the catalysis tests are shown in Figure 2. The three samples initially possessed fine pore/ligament microstructures (20–50 nm), but after heat treatment they showed significant pore/ligament coarsening, and the sizes of the pores/ligaments of the three samples after the tests were all 100–200 nm. It is noteworthy that the as-fabricated NP-Co was oxidized according to STEM-EDS mapping (Figure A1), and the surface of this material was not catalytically active during the reaction. Therefore, surface oxides may hinder the uniform ligament coarsening and cause a bi-modal grain size distribution, as shown in Figure 2d. Figure 3 displays the STEM-EDS maps for Ni, Co, Mn, and O in NP-NiCo before and after the catalysis test. Before the test, the four elements were distributed uniformly and well mixed at the nanoscale, but after the test the residual Mn had been converted to Mn oxides, which are not active materials in DRM. These oxides were distributed on uniform NiCo ligaments that displayed almost perfect yellow in the color-mixing map of Ni and Co, regardless of the oxygen distribution. The NiCo ligaments were also oxidized, as shown by the oxygen map. It is worth noting that static observations alone cannot explain why NP-NiCo, which has a similar pore/ligament size to the other materials, possessed improved activity and thermal stability, as indicated by the catalysis test (Figure 1).

In order to know the origin of the moderate activity and thermal stability of NP-NiCo, we performed an in-situ TEM study of NP-NiCo during DRM. The changes in the microstructure over time are shown in Figure 4. When the temperature was increased up to 600 °C under vacuum, the pore/ligaments coarsened, as expected (Figure 4a). More importantly, the grains in the ligaments became finer when the mixture gas (CH₄ + CO₂) was introduced into the TEM chamber (Figure 4b,c). After this, the mixture gas was evacuated, and the grains tended to merge and form larger grains over a short amount of time, judging from the diffracted contrasts, meaning that the fine features of the demixed elements were thermodynamically unstable. We cooled down the sample within ~5 min, and then performed STEM-EDS analysis of the sample, as shown in Figure 5. The chemical demixing of Ni and Co can be clearly observed regardless of surface oxidation, in addition to the dispersion of MnO₂. This chemical analysis suggests that the DRM reaction induced chemical demixing accompanied by the fine grains of Ni and Co working as additional active sites at high temperatures. No carbon deposition was observed in the throughout in-situ observation. However, it should be noted that these unique features could only be observed by in-situ TEM, because the catalysis test usually requires ~30 min to cool down to room temperature in order to protect the reaction system as rapid cooling may break the

quartz tube and then expose the residual CO to air. Therefore, chemical demixing was not observed after the conventional catalysis test (Figure 3). This chemical demixing and grain refinement could also imply “synergic effects” similar to those seen in previous studies, which have shown higher catalytic activity and durability of bimetallic Ni–Co compared to Ni [17,18].

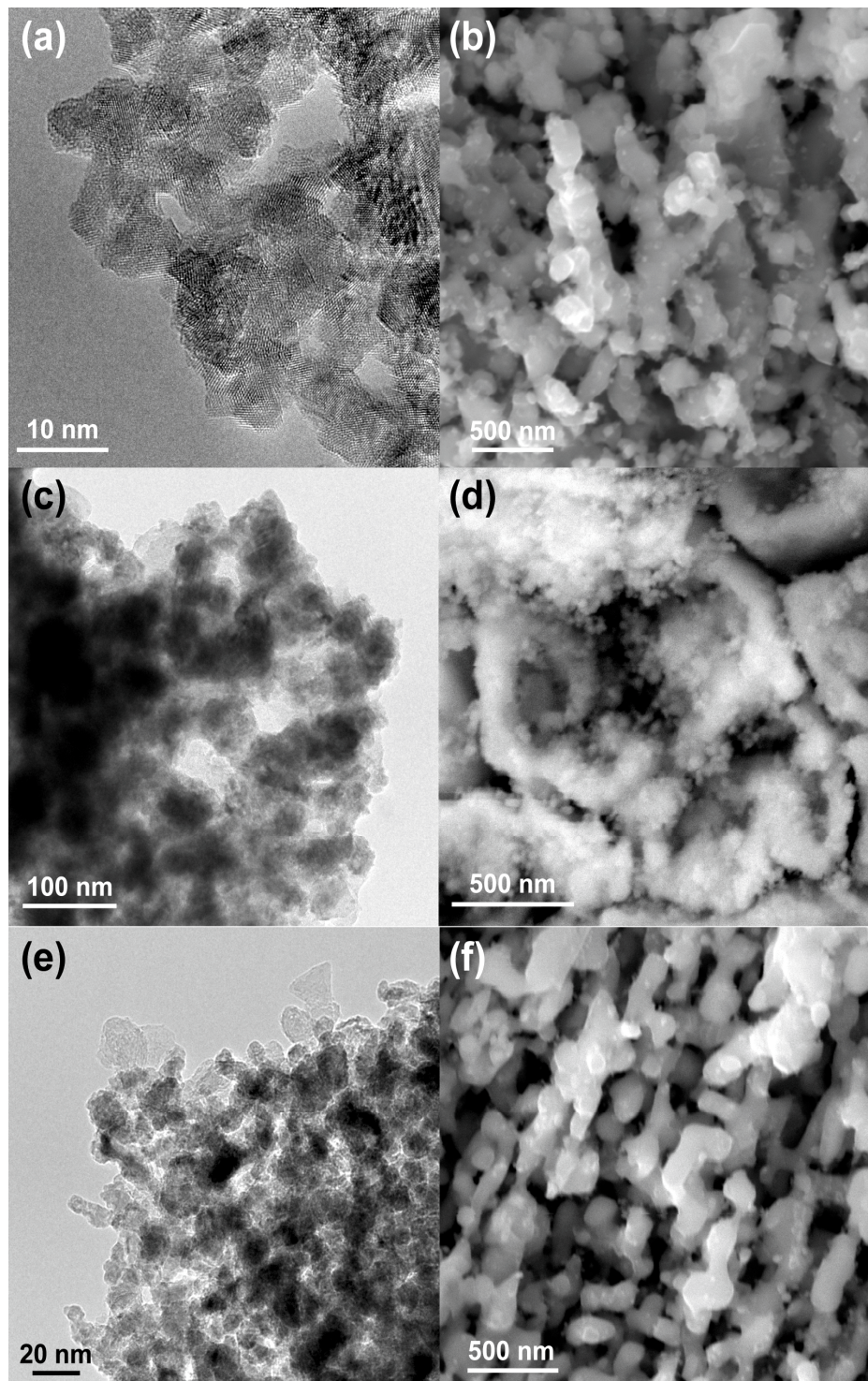


Figure 2. Microstructure observations taken by SEM or TEM before (a,c,e) and after (b,d,f) the catalysis tests; (a,b) NP-Ni; (c,d) NP-Co; and (e,f) NP-NiCo.

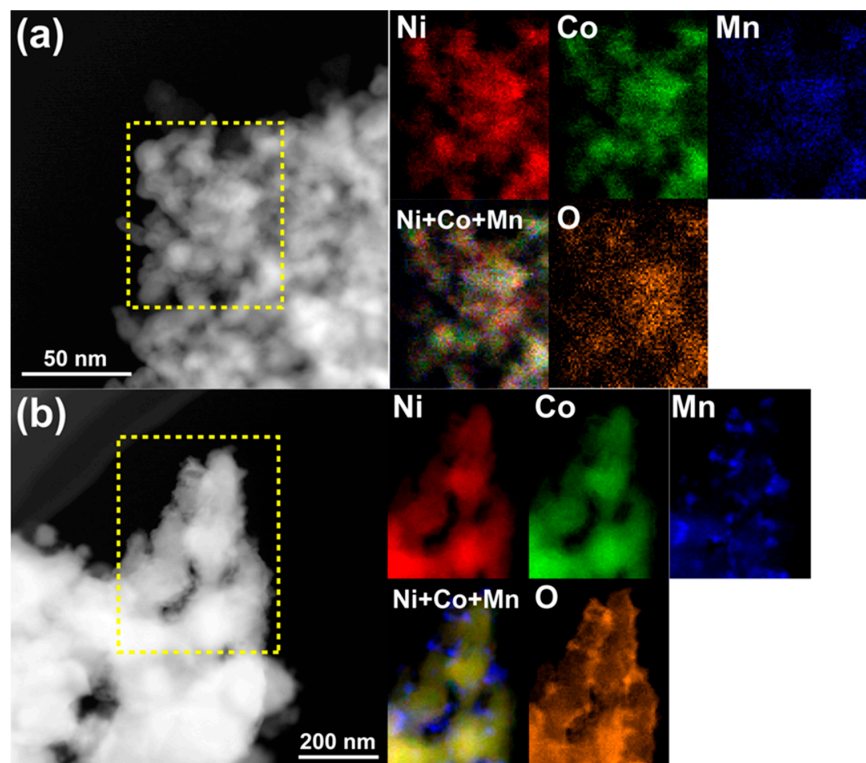


Figure 3. STEM images and energy dispersive X-ray spectrometry (EDS) chemical maps of the highlighted areas showing the distributions of Ni (red), Co (green), Mn (blue), and O (orange) from Ni-K, Co-K, Mn-K, and O-K, respectively, in NP-NiCo (a) before the catalysis test and (b) after the test. Combined images of Ni, Co, and Mn are also shown.

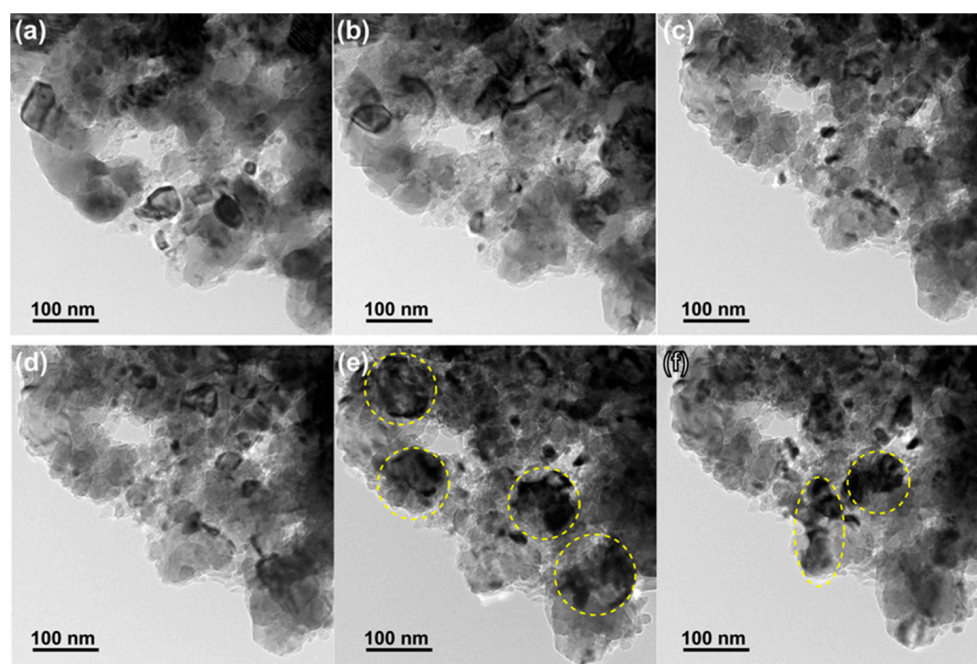


Figure 4. Microstructure evolution as observed by in-situ TEM. Images taken: (a) after temperature reached 600 °C under vacuum; (b,c) after 5 and 10 min of exposure to the gas mixture, respectively; (d) just after evacuation of the gas mixture; (e,f) during cooling to room temperature under vacuum. The selected areas indicate coarsened grains during cooling.

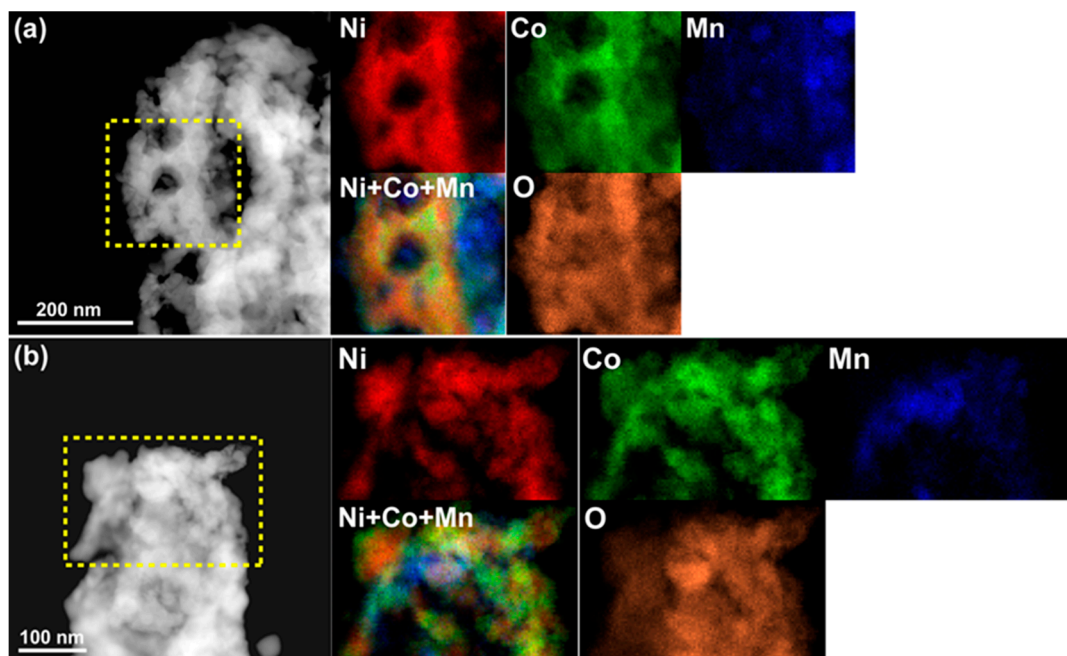


Figure 5. STEM images and EDS chemical maps of NP-NiCo after the in-situ TEM study. The selected areas in two different places (**a,b**) show the heterogeneous distributions of Ni (red), Co (green), Mn (blue), and O (orange) from Ni-K, Co-K, Mn-K, and O-K, respectively.

The chemical demixing may originate from the different reaction affinities of the metal and reactant species at high energy states. For example, solid-solution Pd-Co alloys show chemical demixing of Pd and Co by microwave H₂ irradiation [19], indicating the different elemental interactions with H₂. Similarly, Ni and Co have different affinities to DRM: Ni is active but Co is inert; thus, this situation promotes the elemental separation, resulting in grain refinement.

4. Conclusions

In summary, we employed in-situ TEM during DRM using NP-NiCo to investigate its catalytic activity and durability. From the in-situ observations and chemical analysis, we concluded that DRM induces chemical demixing of Ni and Co accompanied by grain refinement, giving rise to important “synergic effects” similar to those reported for bimetallic catalysts in previous studies. Even though the thermal stability in NP-NiCo was improved over those of single component catalysts, there is still further room for improvement, as Co is an inert element and therefore sacrifices the performance for thermal stability. We will keep examining other elements in our attempts to fulfil the need for both high activity and durability, as we hope to find a more suitable inert element to act as a structural backbone in DRM reactions for future work.

Acknowledgments: This study was mainly supported by the JST-CREST program “Innovative catalysts and creation technologies for the utilization of diverse natural carbon resources” (grant No. JPMJCR15P1) and research funds provided by the “World Premier International (WPI) Research Center Initiative for Atoms, Molecules and Materials”, MEXT (Japan). It was also partially supported by KAKENHI (grant No. JP16H02293). We also acknowledge the support from the Advanced Characterization Nanotechnology Platform of the High Voltage Electron Microscope Laboratory at Nagoya University.

Author Contributions: Takeshi Fujita fabricated samples, conducted TEM/STEM characterizations, and performed catalysis test. Takeshi Fujita, Kimitaka Higuchi, Yuta Yamamoto, Tomoharu Tokunaga, Shigeo Arai and Hideki Abe performed in-situ TEM observations. Takeshi Fujita conducted the study design, data analysis, and data interpretation. Takeshi Fujita wrote the paper. Takeshi Fujita and Hideki Abe contributed to this work through the direction of the research.

Conflicts of Interest: The authors declare no conflict of interest.

Appendix A

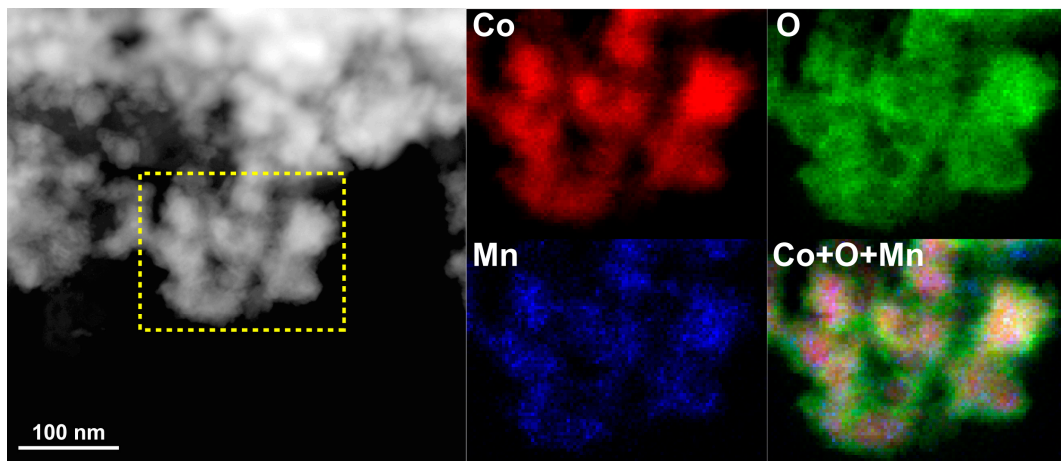


Figure A1. STEM image and EDS chemical maps of as-fabricated NP-Co before the in-situ TEM study. The selected area shows the distributions of Co (red), O (green), and Mn (blue) from Co-K, O-K, and Mn-K, respectively. The surface of the Co ligament was clearly oxidized.

References

- Muraza, O.; Galadima, A. A review on coke management during dry reforming of methane. *Int. J. Energy Res.* **2015**, *39*, 1196–1216. [[CrossRef](#)]
- Nair, M.M.; Kaliaguine, S. Structured catalysts for dry reforming of methane. *New J. Chem.* **2016**, *40*, 4049–4060. [[CrossRef](#)]
- Lavoie, J.M. Review on dry reforming of methane, a potentially more environmentally-friendly approach to the increasing natural gas exploitation. *Front. Chem.* **2014**, *2*, 81. [[CrossRef](#)] [[PubMed](#)]
- Ding, Y.; Chen, M.W. Nanoporous metals for catalytic and optical applications. *MRS Bull.* **2009**, *34*, 569–576. [[CrossRef](#)]
- Qiu, H.J.; Li, X.; Xu, H.T.; Zhang, H.J.; Wang, Y. Nanoporous metal as a platform for electrochemical and optical sensing. *J. Mater. Chem. C* **2014**, *2*, 9788–9799. [[CrossRef](#)]
- Qiu, H.J.; Xu, H.T.; Liu, L.; Wang, Y. Correlation of the structure and applications of dealloyed nanoporous metals in catalysis and energy conversion/storage. *Nanoscale* **2015**, *7*, 386–400. [[CrossRef](#)] [[PubMed](#)]
- Juarez, T.; Biener, J.; Weissmüller, J.; Hodge, A.M.C. Nanoporous metals with structural hierarchy: A review. *Adv. Eng. Mater.* **2017**, in press. [[CrossRef](#)]
- Fujita, T. Hierarchical nanoporous metals as a path toward the ultimate three-dimensional functionality. *Sci. Technol. Adv. Mater.* **2017**, in press.
- Biener, J.; Biener, M.M.; Madix, R.J.; Friend, C.M. Nanoporous gold: Understanding the origin of the reactivity of a 21st century catalyst made by pre-columbian technology. *ACS Catal.* **2015**, *5*, 6263–6270. [[CrossRef](#)]
- Fujita, T.; Tokunaga, T.; Zhang, L.; Li, D.W.; Chen, L.Y.; Arai, S.; Yamamoto, Y.; Hirata, A.; Tanaka, N.; Ding, Y.; et al. Atomic observation of catalysis-induced nanopore coarsening of nanoporous gold. *Nano Lett.* **2014**, *14*, 1172–1177. [[CrossRef](#)] [[PubMed](#)]
- Fujita, T.; Abe, H.; Tanabe, T.; Ito, Y.; Tokunaga, T.; Arai, S.; Yamamoto, Y.; Hirata, A.; Chen, M.W. Earth-abundant and durable nanoporous catalyst for exhaust-gas conversion. *Adv. Funct. Mater.* **2016**, *26*, 1609–1616. [[CrossRef](#)]
- Qiu, H.J.; Kang, J.L.; Liu, P.; Hirata, A.; Fujita, T.; Chen, M.W. Fabrication of large-scale nanoporous nickel with a tunable pore size for energy storage. *J. Power Sources* **2014**, *247*, 896–905. [[CrossRef](#)]
- Tanaka, N.; Usukura, J.; Kusunoki, M.; Saito, Y.; Sasaki, K.; Tanji, T.; Muto, S.; Arai, S. Development of an environmental high-voltage electron microscope for reaction science. *Microscopy* **2013**, *62*, 205–215. [[CrossRef](#)] [[PubMed](#)]

14. Oyama, S.T.; Hacarlioglu, P.; Gu, Y.; Lee, D. Dry reforming of methane has no future for hydrogen production: Comparison with steam reforming at high pressure in standard and membrane reactors. *Int. J. Hydrogen Energy* **2012**, *37*, 10444–10450. [[CrossRef](#)]
15. Ruckenstein, E.; Wang, H.Y. Carbon deposition and catalytic deactivation during CO₂ reforming of CH₄ over CO₂/γ-Al₂O₃ catalysts. *J. Catal.* **2002**, *205*, 289–293. [[CrossRef](#)]
16. Xu, J.K.; Zhou, W.; Li, Z.J.; Wang, J.H.; Ma, J.X. Biogas reforming for hydrogen production over nickel and cobalt bimetallic catalysts. *Int. J. Hydrogen Energy* **2009**, *34*, 6646–6654. [[CrossRef](#)]
17. Ay, H.; Uner, D. Dry reforming of methane over CeO₂ supported Ni, Co and Ni-Co catalysts. *Appl. Catal. B Environ.* **2015**, *179*, 128–138. [[CrossRef](#)]
18. Li, L.D.; Anjum, D.H.; Zhu, H.B.; Saih, Y.; Laveille, P.V.; D’Souza, L.; Basset, J.M. Synergetic effects leading to coke-resistant NiCo bimetallic catalysts for dry reforming of methane. *ChemCatChem* **2015**, *7*, 427–433. [[CrossRef](#)]
19. Tokunaga, T.; Hayashi, Y.; Fujita, T.; Silva, S.R.P.; Amaralunga, G.A.J. Demixing of solid-soluted Co-Pd binary alloy induced by microwave plasma hydrogen irradiation technique. *Jpn. J. Appl. Phys.* **2006**, *45*, L860–L863. [[CrossRef](#)]



© 2017 by the authors. Licensee MDPI, Basel, Switzerland. This article is an open access article distributed under the terms and conditions of the Creative Commons Attribution (CC BY) license (<http://creativecommons.org/licenses/by/4.0/>).